Infra-slow modulation of fast beta/gamma oscillations in the mouse visual system.

Patrycja Orlowska-Feuer[1a*], Annette Elisabeth Allen[2], Timothy Matthew Brown[3], Hanna Jowita Szkudlarek[1b], Robert James Lucas[3], Riccardo Storchi[2*]

Affiliations:
[1] Department of Neurophysiology and Chronobiology, Institute of Zoology and Biomedical Research, Jagiellonian University in Krakow, 30-387 Krakow, Poland
[2] Division of Neuroscience and Mental Health, Faculty of Biology Medicine and Health, University of Manchester, M13 9PT Manchester, UK
[3] Centre for Biological Timing, Faculty of Biology, Medicine and Health, University of Manchester, M13 9PT Manchester, UK
[a] POF present address: Division of Neuroscience and Mental Health, Faculty of Biology Medicine and Health, University of Manchester, M13 9PT Manchester, UK
[b] HJS present address: Department of Anatomy and Cell Biology, Medical Science Bldg, University of Western Ontario, London, ON, Canada

* Corresponding authors
Riccardo Storchi, PhD
riccardo.storchi@manchester.ac.uk
Patrycja Orlowska-Feuer, PhD
patrycja.orlowska@uj.edu.pl

Abbreviated title: Oscillatory activities in the subcortical visual system.
Number of pages:
Number of figures: 7
Number of tables: 3
Number of words for Abstract:
Number of words for Introduction:
Number of words for Discussion:

Conflict of interest statement
The authors declare no competing financial interests.

Acknowledgment
The work of POF was partially supported by the Bekker Programme implemented by the Polish National Agency for Academic Exchange. RS was funded by National Centre for Replacement Refinement and Reduction of Animals in Research (NC3Rs) via a David Sainsbury Fellowship (NC/P001505/1). RJL was funded by The Wellcome Trust (Investigator Award 210684/Z/18/Z) and The European Research Council (268970).

Authors contribution
POF, HJS, RJL, RS designed research; POF, AEA, TMB performed research; RS contributed analytic tools; POF, HJS, RS analyzed data; POF, RJL, RS interpreted the results; POF, RJL, RS wrote the paper.

ABSTRACT

Infra-slow (<0.01Hz) and fast beta/gamma (15 – 60 Hz) oscillations in neurophysiological activity have been widely found in the subcortical visual system. While it is well established that fast beta/gamma oscillations are involved in visual processing the role (if any) of infra-slow oscillations is currently unknown. In this study we tested the possibility that infra-slow oscillations affect visual processing by modulating fast beta/gamma oscillations.

We recorded spontanous activity *in vivo* from the mouse subcortical visual system. We found that in neurons expressing both rhythms the phase of infra-slow modulates the amplitude of fast beta/gamma oscillations. Moreover the level of co-expression of these rhythms was substantially above chance suggesting that these rhythms are functionally linked. To further investigate infra-slow and fast beta/gamma coupling we asked whether its emergence was contingent upon intact rod/cone and melanopsin photoreception. In animals with non-functional rod/cone vision fast beta/gamma were abolished while infra-slow were potentiated indicating that infra-slow and fast beta/gamma are distinct events. In animals with genetic deletion of melanopsin both rhythms were expressed but their interaction was substantially disrupted.

Together our results indicate that infra-slow oscillations are separable phenomena tied together by vision. Thus under physiological conditions infra-slow modulate fast beta/gamma oscillations through a sizeable population of neurons expressing both rhythms.

SIGNIFICANCE STATEMENT

Neurophysiological activity in the subcortical visual system fluctuates in both infra-slow and fast oscillatory ranges, however the level of co-occurrence and potential functional interaction of these rhythms is unknown. Analyzing spontaneous activity in the mouse subcortical visual system, we find that these two types of oscillation interact uniquely through a population of neurons expressing both rhythms. Genetic ablation of rod/cone signaling potentiates infra-slow and abolishes fast beta/gamma oscillations while genetic ablation of melanopsin substantially diminishes the interaction between these two rhythms. Thus our results indicate that in an intact visual system infra-slow modulate fast beta/gamma oscillations. For this modulation to emerge outer and inner retina photoreception are both required and play different roles.

INTRODUCTION

Regular infra-slow (< 0.01Hz) oscillations in neurophysiological activity have been found throughout the mammalian visual system, including the retina (Rodieck and Smith, 1966), optic chiasm (Cavaggioni, 1968), the dorsal lateral geniculate nucleus (dLGN) (Albrecht and Gabriel, 1994; Albrecht et al., 1998), ventral lateral geniculate nucleus (vLGN) (Chrobok et al., 2018), olivary pretectal nucleus (OPN) (Szkudlarek et al., 2008, 2012), suprachiasmatic nucleus (SCN) (Aggelopoulos and Meissl, 2000), intergeniculate leaflet (IGL) (Lewandowski et al., 2000, 2002) and primary visual cortex (Filippov and Frolov, 2005). Infra-slow oscillatory rhythm features such as the frequency and amplitude are modulated by light (Miller and Fuller, 1992; Albrecht et al., 1998; Lewandowski et al., 2000; Szkudlarek et al., 2012). Nevertheless, despite its ubiquity, the contribution of such rhythmicity to visual processing, if at all significant, is still a matter of debate.

Oscillations at a quite different frequency range (15 – 60 Hz, termed beta/gamma) are also a feature of the early visual system. Such oscillations have been implicated in different aspects of visual processing ranging from inter-area communication to feature binding (Gray et al., 1989; Fries, 2005). Recently, we and others also reported that the power of fast beta/gamma oscillations encodes for ambient light intensity and spatially structured changes in luminance (Saleem et al., 2017; Storchi et al., 2017).

Decades of research have highlighted a general organizing principle by which the brain orchestrates oscillations expressed at different timescales. Namely faster oscillations are "nested" within slower oscillations so that the power of faster oscillations is controlled by the phase of the slower ones. Remarkable example of this phenomenon is the theta-gamma coupling in the hippocampus that has been shown to underlie spatial navigation and object memory recollection (Lisman and Jensen, 2013; Gupta et al., 2016). Electroencephalographic recordings in humans indicates that also infra-slow oscillations can modulate faster rhythms (Vanhatalo et

al., 2004a; Monto et al., 2008). Thus one possible impact of infra-slow oscillations in vision is to guide visual processing by interacting with fast narrowband oscillations.

To test this possibility we recorded from mouse subcortical visual system (dLGN, vLGN and OPN). We found that infra-slow and fast beta/gamma oscillations interact through a population of neurons that co-express both rhythms. Namely in these neurons the phase of infra-slow modulates the amplitude of gamma. We then asked whether this interaction required intact vision by repeating the same experiments in animals with genetic ablation of rods+cones or melanopsin photoreception. We found that rod+cone loss abolished fast oscillations, but left infra-slow rhythms intact, whereas both oscillations were retained in melanopsin knockouts but their co-expression was substantially reduced. Together these results confirm that infra-slow and fast oscillations are separable phenomena reflecting different network states, and also that in physiological conditions their co-expression in the same neurons is an active consequence of a particular network state that is disrupted by melanopsin loss.

MATERIALS AND METHODS

Ethical approval

All procedures involving animals were carried out in accordance with regulations and standards of the European Community Council Directive of 24 November 1986 (86/609/EEC) and approvals of the institutional ethics committee and the UK Home Office.

The following report is in part a re-analysis of previously collected and partially published elsewhere data (Brown et al., 2010; Allen et al., 2011).

Animals

Experiments were performed on genetically modified mice (n = 61) which were bred in the animal facility of the Faculty of Life Sciences at Manchester University, UK. Animals were

housed under standard conditions (60% of humidity and food and water *at libitum*) with 12:12 h light/dark cycle. Animals were 3 - 5 months old males with three different genetic backgrounds: *Opn1mw*^{R} mice (C57BL/6:129sv strain) had all types of photoreceptors functional; rodeless and coneless (*rd/rd cl)* mice (C3H strain) lacked rods and cones and *Opn4*$^{-/-}$ mice (C57BL/6:129sv strain) lacked melanopsin. *Opn1mw*^{R} mice had a medium wavelength-sensitivity (MWS) opsin replaced by human red opsin, what shifted cone spectral sensitivity but had no other known effects on retinal functions and connectivity (Smallwood et al., 2003; Jacobs and Williams, 2007). Due to that fact *Opn1mw*^{R} mice were used as 'wild type' animals. Animals were removed from their home cages at the beginning of the projected day and the electrophysiological recordings spanned the mid portion of the day.

Surgery

All surgical procedures were conducted under deep urethane anesthesia (1.55 g / kg, 30% w / v; Sigma-Aldrich, Munich, Germany). Animals were injected intraperitoneally and the depth of anesthesia was ascertained by lack of withdrawal and ocular reflexes. If necessary, animals were supplemented with 10% of the initial dose of urethane. Body temperature was automatically maintained at 37 ± 0.5°C by the thermistor with a feedback-controlled heating pad. Anesthetized mice were carefully placed in a stereotaxic frame via ear bars (SR-15M, Narishige International Limited, London, UK). Skin and all soft tissues covering the skull were removed exposing coronal, sagittal and lambdoid sutures. Next, bregma point was determined and craniotomy was performed above the OPN or LGN. The coordinates were assessed based on a stereotaxic brain atlas for mice (Paxinos & Franklin, 2001) and were AP, -2.8; LM, 0.9; DV, -2 to -2.8 mm and AP, -2.5; LM, 2.2; DV, 2.5 to 3.5 mm for the OPN and LGN, respectively.

Electrophysiology

A 32-channel multiunit electrode array (A4X8-5 mm-50-200-413; NeuroNexus Technologies, Dallas, TX, USA) was used to record neuronal activities from the pretectum and LGN area. It consisted of 4 silicon shanks (spaced 200 µm), each with 8 recordings sites spaced vertically at 50 µm. Neuronal signals were acquired using Recorder64 system (Plexon, Dallas, TX, USA). Signals were amplified (3000×), filtered (300 Hz) and digitized at 40 kHz. All data were saved on a computer hard disc for further analysis.

A 4 × 8 electrode array was introduced to a 350 × 600 µm area of the pretectum or LGN and recordings were taken regardless of types of recorded activities (oscillatory or non-oscillatory) in dark adapted conditions. Moreover, recordings in some animals were not limited to one penetration.

Histological verification

Prior to the first insertion, the electrode was dipped in fluorescent dye (Cell Tracker CM-Dil, Invitrogen Ltd., UK) in order to verify position of all recording places. At the end of the experiment animals were intracardially perfused with a buffered physiological saline followed by 4% paraformaldehyde in 0.1 M phosphate buffer (pH = 7.2). Brains were removed from the skull and postfixed overnight in the same fixative at 4°C. Cryoprotected brains (immersion in 30% sucrose solution for 2-3 days) were cut on a freezing microtome at a coronal plane. Sequential sections (100 µm thick) with CM-Dil depositions were mounted on the gelatin-coated glass slides. Sections were carefully inspected, photographed and ascribed to a related coronal plain of the brain according to the stereotaxic atlas of a mouse brain (Paxinos & Franklin, 2001). Expression of the parvalbumin (calcium binding protein) was used as the marker of OPN neurons (for the precise description of the method see Allen et al., 2011). The optic tract, hippocampus and third ventricle were used as landmarks to determine the LGN borders.

Data analysis

Multi-unit recordings were processed using Offline Sorter (version 2.8.8; Plexon) or Spike2 (version 6.08). After removal cross-channel artifacts, each channel was analyzed separately. Single-units were detected and categorized based on spike waveform via principal component analysis (PCA) and related statistic. Moreover, the inter-spike interval (ISI) histograms were computed to monitor unit refractory period.

The oscillatory activity in the infra-slow (≤ 0.01 Hz) and beta/gamma (15 – 60 Hz, through the manuscript called fast, as it was shown that gamma frequency is tunable by the depth of anesthesia and here we only recorded from urethane anaesthetized animals (Storchi et al., 2017)) range were assessed based on the generated rate-meter histograms (1 s bins, 900 – 1100 s long epochs, recorded under dark-adapted condition). The Fast Fourier Transform (FFT) analysis was applied to estimate the infra-slow frequency. Fast oscillatory activity was determined based on the Power Spectral Density (PSD) function and multi-modal distribution of ISI histograms (Tsuji et al., 2016). The amplitude of the PSD was normalized to a raw PSD and a Hamming window function was used.

A cross correlation function was estimated between all pairs of units simultaneously recorded. For each pair a cross-correlation index was then obtained by calculating the median of the cross-correlation function in the interval (-10, 10) seconds. To test whether this index was significantly different from zero we applied a sign-test at the distribution of cross-correlation indexes.

Estimation of coupling between infra-slow and fast beta/gamma oscillations

For these analyses the timestamps of simultaneously recorded neurons expressing infra-slow, fast beta/gamma or both oscillations were pooled together. Spike timestamps were binned at 1 s for infra-slow and 2 ms for fast beta/gamma to obtain spike counts. Those counts were filtered by using zero-phase Kaiser filters (infra-slow: low pass filter with cut-off at 0.1 Hz and stop-band at 0.05 Hz; fast beta/gamma: pass band filter with cut-off at ±5 Hz from narrowband peak

and stop-band at ±10 Hz). A Hilbert transformation was then applied to the spike counts filtered in the infra-slow range and the phase of these signals was clipped in the range (-π, π). Finally the phase of infra-slow spike counts was used to divide fast beta/gamma band spike counts into the intervals ((0, π/2); (π/2, π); (0, -π/2); (-π/2, -π)). In order to test against the possibility that the amplitude of fast beta/gamma oscillations is modulated by the phase of infra-slow oscillations we compared the amplitude of these oscillations in the range (-π, 0) with the amplitude observed in the range (0, π) by using a sign-test.

Permutation Test

Permutation test was used to test the null hypothesis that occurrence of fast and infra-slow oscillations at the level of individual units were statistically independent events. First we counted the actual number of units expressing both fast and infra-slow rhythms. Then we compared those numbers with a null distribution obtained using the following simple permutation technique. First, for each recording, we generated a binary N-by-2 matrix were each row represented an individual unit, the first column reported presence (or absence) of infra-slow oscillations (presence = 1; absence = 0) and the second column presence (or absence) of fast oscillations. Then, in order to break statistical dependence between these oscillations, we performed a random permutation of one of those columns. Finally, we calculated the number of units co-expressing both rhythms (equivalent to a logical AND). Since different realization of a random permutation can produce different results we estimated the null distribution by repeating this procedure 10000 times. An example is shown in Table 1.

Statistical Comparisons

Statistical comparisons of the means ± SD were performed using non-parametrical Kruskal-Wallis test or Friedman test (followed by Dunn's Multiple Comparison Test). The sampling distribution was verified with Chi-square test. A probability error of $P < 0.05$ was regarded as significant. All data were visualized and statistically examined using Office Excel (2003;

Microsoft Corporation), GraphPad (version 4.02; GraphPad Software), NeuroExplorer (version 5; Nex Technologies), Statistica software (StatSoft, Inc., Tulsa, Oklahoma, USA) and scripts written in MATLAB (R2019a).

Codes Accessibility

The original dataset in .csv format and MATLAB codes for replicating the tests are available from the corresponding authors on reasonable requests.

RESULTS

The main aim of this work was to determine the relationship between infra-slow and fast narrowband oscillations in the mouse visual system. We addressed these questions both in image forming and in non-image forming centres in the brain by focussing on the dLGN (image forming), vLGN and OPN (both non-image forming structures).

Infra-slow oscillations are widespread in the mouse visual system & co-exist with fast narrowband rhythms

Infra-slow oscillations have been observed in many species including rats, cats and monkeys but not previously in mice. Therefore, we first aimed to verify the occurrence of infra-slow oscillatory activity (<0.01 Hz) in the spontaneous neuronal firing in the subcortical visual system of mouse. We unbiasedly recorded in the absence of visual input (in darkness) from the OPN, dLGN and vLGN in visually intact *Opn1mw*^{R} mice.

The FFT analysis revealed that ~30% of all recorded units expressed an infra-slow oscillatory rhythm (<0.01 Hz) in spiking activity, resembling previously reported oscillations in the rat subcortical visual system (Albrecht and Gabriel, 1994; Lewandowski et al., 2000; Szkudlarek et al., 2008; Chrobok et al., 2018). In Fig.1 examples of rhythmically firing units in the OPN, dLGN and vLGN are presented. The mean frequency of observed oscillations ranged between 0.0033 and 0.0117 Hz and did not differ between structures (Kruskal-Wallis test, K-W statistics = 5.743, p = 0.056; Fig. 1E). The proportion of infra-slow oscillatory neurons was also indistinguishable among these nuclei (33%, 29% and 31% in the OPN, dLGN and vLGN, respectively; Chi-square test, p = 0.7546, Chi-square = 0.5631, df = 2). In the same dataset described in Fig.1 we found that a fraction of neurons expressed fast narrowband oscillations in the beta/gamma range (15 – 60 Hz). A power spectra density (PSD) analysis and multimodal distribution of peaks at the level of ISI histograms of spontaneous spike activity revealed that

32% (OPN), 9% (dLGN) and 19% (vLGN) of all recorded units expressed such fast oscillations under dark-adapted condition. The frequency of these oscillations averaged at 34.94 ± 5.02 Hz (OPN), 31.02 ± 7.57 Hz (dLGN) and 25.27 ± 7.63 Hz (vLGN) (Fig. 2). In contrast to infra-slow oscillatory activity, the frequency and proportion of fast units differed between structures (Kruskal-Wallis test, $P < 0.0001$, K-W statistic = 22.12, Dunn's multiple comparison test; Chi-square test, $p<0.0001$, Chi-square = 37.15, df = 2).

Based on that data we were able to describe four types of spontaneous activity (in darkness) in the sub-cortical visual system of visually intact mice: infra-slow or fast oscillatory activity alone; co-expression of both rhythms; and no oscillatory activity in the above ranges (Fig. 3). Co-expression of infra-slow and fast oscillations were found in 12%, 5% and 17% of all OPN, dLGN and vLGN neurons, respectively (Chi-square test, $p<0.0001$, Chi-square value = 22.01, df = 2, Fig. 3E). Firing rate of neurons expressing only infra-slow were significantly correlated between each other in all the structures investigated (Table 2 for *Opn1mw*^{R}) as revealed by the cross-correlation analysis (see Material and Methods section). Significant correlations were also observed in neurons co-expressing both infra-slow and fast oscillations (Table 2 for *Opn1mw*^{R}). Moreover, these two populations were significantly correlated with each other (Table 2 for *Opn1mw*^{R}) suggesting that a single infra-slow rhythm coordinates firing rate in both populations.

Fast beta/gamma oscillations are modulated in the infra-slow range by diffuse co-expression of both rhythms at single unit level

We next aimed to investigate the possibility that infra-slow oscillations modulate fast beta/gamma oscillations. We asked how infra-slow and fast oscillations interacted across neurons that were separately expressing those oscillations, and in those neurons in which they were co-expressed. In fact, we found that neurons expressing only fast oscillations were largely

unaffected by the population-level infra-slow oscillations (Fig. 4A,B). By contrast, fast beta/gamma rhythms were strongly modulated according to the phase of infra-slow oscillations in those neurons expressing both oscillations (Fig. 4D,E). These results were consistent across the whole dataset indicating that co-expression of both rhythms at the level of individual unit is required for infra-slow modulation of fast narrowband oscillations (Fig 4C,F).

Finally, we measured the extent to which the expressions of infra-slow and fast oscillations were coordinated at population level. To address this question, we tested the possibility that co-expression of fast and infra-slow oscillations could simply occur by chance. We compared the observed number of units where infra-slow and fast oscillations were co-expressed with the number we would expect under the null hypothesis that these two oscillations were independent (see Permutation Test and Table 1 for details). We first asked whether a statistical dependence between infra-slow and fast oscillations expressing neurons would emerge from the whole. To do so we pooled together all neuronal groups recorded in the dLGN, vLGN and OPN nuclei (Fig. 4G). We found that the number of neurons co-expressing infra-slow and fast oscillations was larger than expected by chance, indicating that these rhythms tended to co-occur at the level of individual units. Results from individual areas (dLGN, vLGN, OPN) were qualitatively the same for the dLGN and vLGN while in OPN co-expression was not significantly higher than chance (Fig. 4G).

Outer and inner retina photoreception play different roles in the control of infra-slow modulation of fast beta/gamma oscillations

The data from visually intact mice thus suggest that infra-slow and fast oscillations are separable phenomena, which nonetheless co-occur more than expected by chance. Previous results indicate that expression of both infra-slow and fast beta/gamma oscillations depends both on outer and inner retina photoreception (respectively rods/cones and melanopsin)

(Orlowska-Feuer et al., 2016a; Storchi et al., 2017; Chrobok et al., 2018). We now employed disruption of these two types of photoreceptor to further explore the inter-dependence of oscillations at high and infra-slow frequency. We repeated our initial experiments in a mouse model of aggressive retinal degeneration, lacking rod and cone photoreceptors at the time of recording (*rd/rd cl;* (Lucas and Foster, 1999; Lucas et al., 1999)), and in mice with a more subtle deficit in retinal function caused by loss of the inner retinal photopigment melanopsin (*Opn4*$^{-/-}$). The detailed analysis of all recorded cells in all genotypes is presented in Table 3.

In both groups of mice we found significant differences in the prevalence and the features of both infra-slow and fast beta/gamma oscillations compared with visually intact animals. The highest percentage of units expressing infra-slow oscillations was observed in *rd/rd cl* (46%, 43% and 34% for the OPN, dLGN and vLGN, respectively), followed by *Opn1mw*^{R} (33%, 29% and 31%), and *Opn4*$^{-/-}$ mice (20%, 20% and 15%). Also the frequency of infra-slow oscillations was significantly different among genotypes. Specifically both *rd/rd cl* and *Opn4*$^{-/-}$ mice exhibited faster infra-slow oscillations compared with visually intact *Opn1mw*^{R} animals and *rd/rd cl* oscillations were significantly faster than *Opn4*$^{-/-}$ (OPN: Kruskal-Wallis test, Kruskal-Wallis statistics = 15.89, $p = 0.0004$; dLGN: Kruskal-Wallis test, Kruskal-Wallis statistics = 32.89, $P < 0.0001$; vLGN: Kruskal-Wallis test, Kruskal-Wallis statistics = 20.80, $P < 0.0001$; Fig. 5).

In *rd/rd cl* mice, in which almost half of the recorded units exhibited infra-slow oscillatory activity, fast oscillations were largely abolished (OPN: 4 out of 98; dLGN: 1 out of 307; vLGN: 0 out of 97). On the other hand, in *Opn4*$^{-/-}$ mice the percentage of units expressing fast oscillations was comparable with visually intact animals (21%, 11% and 17% in the OPN, dLGN and vLGN). However, the frequency of fast oscillations was altered in *Opn4*$^{-/-}$ mice in the OPN (lower in the *Opn4*$^{-/-}$ mice) and vLGN (higher in the *Opn4*$^{-/-}$ mice), but not in dLGN (Fig. 5).

Since both rhythms were retained following melanopsin loss, we next asked whether this modulation had altered the interaction between infra-slow and fast beta/gamma oscillations. Similarly to what we found in visually intact animals, neurons recorded from *Opn4*$^{-/-}$ mice could be classified into four distinct types on the base of their expression of one or either oscillatory activity. Also consistently with the *Opn1mw*^{R} genotype, cross-correlation analysis revealed that in both dLGN and vLGN firing rates were correlated within populations of neurons expressing only infra-slow or both rhythms (Table 2 for *Opn4*$^{-/-}$). However, differently from visually intact animals, the firing rates were not correlated between these two populations (Table 2 for *Opn4*$^{-/-}$). Infra-slow modulation of fast oscillations was observed, but as in visually intact mice, this only occurred in neurons expressing both rhythms (Fig. 6).

Finally we asked whether the rate of co-expression of both oscillations was also preserved. We found that this was not the case since in all nuclei co-expression of infra-slow and fast beta/gamma oscillation was not significantly different from chance level in *Opn4*$^{-/-}$ mice (Fig. 6G). This result indicates that inner retinal photoreception, while not required for co-existence of both rhythms, is necessary for tying these rhythms together and enabling a diffuse modulation of fast beta/gamma oscillation in the infra-slow range.

DISCUSSION

Infra-slow oscillations have been ubiquitously observed in the subcortical visual system, however their function remains poorly understood. Instead fast beta/gamma oscillations are involved in several types of visual processing that include inter-area communication along the visual pathway and feature binding (Gray et al., 1989; Fries, 2005). It was previously shown that gamma rhythm couples with slower rhythms expressed in different brain areas (Vanhatalo et al., 2004b; Monto et al., 2008), thus we asked whether that is also the case with infra-slow oscillatory activity in the subcortical visual system.

We find that these two types of oscillation are distinct phenomena, but that they do co-occur more than expected by chance. Importantly, this co-occurrence allows the phase of infra-slow oscillations to modulate the amplitude of the fast. These findings reveal a potential mechanism by which infra-slow oscillations could regulate the visual flow – by modulating the amplitude of fast beta/gamma oscillations in the mouse visual system.

Infra-slow oscillations are a common feature of subcortical visual systems

Oscillations with the period of minutes were described before in the visual system of adult rats (SCN: Miller & Fuller, 1992; dLGN: Albrecht & Gabriel, 1994; IGL: Lewandowski *et al.*, 2000; OPN: Szkudlarek *et al.*, 2008), cats (optic chiasm: Cavaggioni, 1968; retina: Rodieck and Smith, 1966), rabbits (visual cortex: Aladjalova, 1957) and monkeys (visual cortex: Leopold et al., 2003; LGN: Cheong *et al.*, 2011). Our study is the first to show the existence of infra-slow oscillatory rhythm in mice, where we recorded them in the OPN and in both divisions of LGN. According to the present data, infra-slow oscillatory neurons constitute ~30% of all recorded units in dark adapted mice. For comparison, previous studies have shown that in rats, such neurons constitute 18% and 63% of all cells in the OPN and LGN, respectively (Albrecht and Gabriel, 1994; Szkudlarek et al., 2012). The frequency of observed oscillations is slower

(~0.005 Hz) than those of rats (~0.01 Hz), however, there is no doubt that the pattern of spike generation is the same (Fig.1). Differences between these species in the fraction of neurons expressing infra-slow oscillation and in their frequency could have different potential origins. On one hand, it could be a genuine species difference in visual physiology. On the other, it may be connected to the fact that albino Wistar rats carry several dysfunctions in the visual system (Bolles and Woods, 1964; Lund, 1964; Heiduschka and Schraermeyer, 2008; Nadal-Nicolás et al., 2012) while this study was performed in fully pigmented mice. Finally, it is possible that part of the variability could be simply explained by the small sample sizes used in the previous studies, where single channel recordings were employed as opposed to the higher-yield multichannel electrodes used in this study.

Infra-slow and fast beta-gamma oscillations interact through co-expression of both rhythms at the level of single units

While co-existence of infra-slow and fast beta/gamma has been reported in the subcortical visual system (Tsuji et al., 2016; Chrobok et al., 2018), until now the extent to which they are independent events and whether they interact was unknown. Our data, obtained by unbiased recordings of all active neurons in the dark, reveal that while a subset of cells express only one type of oscillation, others express either both or none (Fig. 3).

In principle, in such population in which not all neurons expressing one type of oscillation also have the other, slow oscillations could still modulate fast beta/gamma oscillations by two types of circuitries. On the one hand, the population of infra-slow neurons could provide a global modulation of beta/gamma oscillations, including neurons that did not themselves have infra-slow oscillations (Fig. 7A). Alternatively, such modulation could be restricted to neurons in which the two types of oscillations could interact within single neurons (Fig. 7B). Our analyses revealed that only neurons co-expressing both oscillations are responsible for mediating infra-

slow modulation of fast beta/gamma oscillations (Fig. 4D-F). That is, when they co-occur the amplitude of fast modulations is modified according to the infra-slow rhythm. Importantly, the level of co-expression of these rhythms was higher than expected by two independent events suggesting that the interaction between infra-slow and fast beta/gamma occurs "by design" rather than simply by chance (Fig. 4G).

Changes to the retinal network alter appearance and interaction of infra-slow and fast oscillations

The retina has been previously implicated in the emergence of both infra-slow and fast oscillations in the sub-cortical brain, with intraocular injection of tetradotoxin abolishing both (Lewandowski and Błasiak, 2004; Szkudlarek et al., 2012; Orlowska-Feuer et al., 2016a, 2016b; Chrobok et al., 2018). Here, we studied rhythmicity in two mice in which the optic nerve was intact and active but in which retinal function was disrupted. These were a model of aggressive photoreceptor degeneration, lacking rod+cone cells (*rd/rd cl* mice), and animals in which inner retina photoreception is ablated (*Opn4*$^{-/-}$ mice). As we were recording activity in the dark, the loss of photoreception in these manipulations is not itself expected to impact our findings, but secondary effects on the retinal circuitry could. Photoreceptors degeneration has knock-on effects on inner-retinal neurons and induces aberrant spontaneous ganglion cell activity in the form of ~10 Hz oscillations (Jones et al., 2003; Ryu et al., 2010; Menzler and Zeck, 2011; Trenholm and Awatramani, 2015), while melanopsin knockout has been reported to impact aspects of retinal development (Renna et al., 2011; Kirkby and Feller, 2013; Rao et al., 2013). Infra-slow oscillations were retained in all genotypes. In fact, they were most prevalent in the *rd/rd cl* (see Table 3), consistent with the simulated effect of reduced retinal input (Zierenberg et al., 2018). Both genetic modifications altered their frequency, and this effect was replicated

across all visual centers, consistent with the view that these infra-slow oscillations share a common mechanistic origin.

The situation with respect to fast beta/gamma oscillations was quite different, with this behavior essentially absent in *rd/rd cl* mice. This dramatic effect highlights the importance of the retinal activity for this rhythm. Since fast beta/gamma oscillations are typically network phenomena (Buzsáki and Wang, 2012), that could be because the retinal circuits generate these oscillations (Kenyon et al., 2003); that interplay between central and retinal circuits is required to produce this rhythmicity; or that the change in retinal input to the brain alters the activity of central circuits generating this rhythmicity.

Perhaps the most interesting alteration in oscillatory activity in transgenic mice was the effective decoupling of infra-slow and fast oscillations in melanopsin knockout animals. While in intact animals these two rhythms co-occurred in individual neurons more often than chance, this property was lost in the *Opn4*$^{-/-}$ genotype. Although we can only speculate as to the change in retinal circuitry responsible for this disruption, it does reinforce the conclusion that the co-occurrence of these oscillations in visually intact animals is an active process. It also provides a new potential mechanism via which this inner retinal photoreceptor typically associated with sub-conscious reflex responses to light could contribute to conventional visual function.

A potential role for the interaction between infra-slow and fast beta/gamma oscillations

In considering the potential function of these two types of oscillation it is important to remember that they have very different spatiotemporal topology. Infra-slow fluctuations are sustained events that can last minutes/hours and are correlated between different brain areas (Szkudlarek et al., 2008; Chrobok et al., 2018). Infra-slow oscillations have also been closely associated with Resting State Networks (RSNs) observed in human fMRI recordings (Damoiseaux et al., 2006; De Luca et al., 2006; He et al., 2008), and most likely reflect the

underlying structural connectivity (Fox and Raichle, 2007; Honey et al., 2007). Fast beta/gamma oscillations typically are short-lasting events that can arise locally and transiently synchronize distant brain areas (Buzsáki, 2006). Those oscillations can be evoked by sensory stimulation (Gray et al., 1989; Cardin et al., 2009; Storchi et al., 2017) or by cognitive tasks (Fries, 2005) but can also emerge spontaneously (Tsuji et al., 2016; Chrobok et al., 2018; Foik et al., 2018). Thus, their spatiotemporal topology is more flexible and need not necessarily reflect the underlying structural connectivity. Accordingly, the interaction between infra-slow and fast beta/gamma could represent a "balancing act" between the opposing needs for transient "on-demand" flexibility – served by fast beta/gamma oscillation – and long-term structural and dynamical stability – served by infra-slow oscillations.

Viewed from this perspective, the strong modulation of fast beta/gamma amplitude by infra-slow oscillations observed here could represent a mechanism to oppose runaway plasticity (Abbott and Nelson, 2000) and promote the stability of visual signaling. This control would then be significantly reduced in *Opn4*$^{-/-}$ animals since these two rhythms are independently expressed within the subcortical visual networks. Consistent with this possibility a previous work showed that light modulation of fast beta/gamma oscillations is substantially reduced in *Opn4*$^{-/-}$ animals (Storchi et al., 2017). Thus, although fast beta/gamma could be observed in the dLGN of *Opn4*$^{-/-}$ animals, these oscillations were less controllable by the visual stimulus. This lack in controllability could be due to the lack of the stabilizing action of infra-slow oscillations.

References

Abbott LF, Nelson SB (2000) Synaptic plasticity: taming the beast. Nat Neurosci 3:1178–1183.

Aggelopoulos NC, Meissl H (2000) Responses of neurones of the rat suprachiasmatic nucleus to retinal illumination under photopic and scotopic conditions. J Physiol 523 Pt 1:211–222

Albrecht D, Gabriel S (1994) Very slow oscillations of activity in geniculate neurons of urethane anaesthetized rats

Albrecht D, Royl G, Kaneoke Y (1998) Very slow oscillatory activities in lateral geniculate neurons of freely moving and anesthetized rats. Neurosci Res 32:209–220.

Allen AE, Brown TM, Lucas RJ (2011) A distinct contribution of short-wavelength-sensitive cones to light-evoked activity in the mouse pretectal olivary nucleus. J Neurosci 31:16833–16843.

Bolles RC, Woods PJ (1964) The ontogeny of behaviour in the albino rat. Anim Behav 12:427–441.

Brown TM, Gias C, Hatori M, Keding SR, Semo M, Coffey PJ, Gigg J, Piggins HD, Panda S, Lucas RJ (2010) Melanopsin contributions to irradiance coding in the thalamo-cortical visual system. PLoS Biol 8.

Buzsáki G (2006) Rhythms of the Brain.

Buzsáki G, Wang X-J (2012) Mechanisms of Gamma Oscillations. Annu Rev Neurosci 35:203–225.

Cardin JA, Carlén M, Meletis K, Knoblich U, Zhang F, Deisseroth K, Tsai LH, Moore CI (2009) Driving fast-spiking cells induces gamma rhythm and controls sensory responses. Nature 459:663–667.

Cavaggioni a. (1968) The dark-discharge of the eye in the unrestrained cat. Pflügers Arch Eur J Physiol 304:75–80.

Cheong SK, Tailby C, Martin PR, Levitte JB, Solomona SG (2011) Slow intrinsic rhythm in the koniocellular visual pathway. Proc Natl Acad Sci U S A 108:14659–14663.

Chrobok L, Palus-Chramiec K, Jeczmien-Lazur JS, Blasiak T, Lewandowski MH (2018) Gamma and infra-slow oscillations shape neuronal firing in the rat subcortical visual system. J Physiol 11:2229–2250.

Damoiseaux JS, Rombouts S a. RB, Barkhof F, Scheltens P, Stam CJ, Smith SM, Beckmann CF (2006) Consistent resting-state networks across healthy subjects. Proc Natl Acad Sci 103:13848–13853.

De Luca M, Beckmann CF, De Stefano N, Matthews PM, Smith SM (2006) fMRI resting state networks define distinct modes of long-distance interactions in the human brain. Neuroimage 29:1359–1367.

Filippov I V., Frolov VA (2005) Very slow potentials in the lateral geniculate complex and primary visual cortex during different illumination changes in freely moving rats. Neurosci Lett 373:51–56.

Foik AT, Ghazaryan A, Waleszczyk WJ (2018) Oscillations in Spontaneous and Visually Evoked Neuronal Activity in the Superficial Layers of the Cat's Superior Colliculus. Front Syst Neurosci 12:1–19.

Fox MD, Raichle ME (2007) Spontaneous fluctuations in brain activity observed with functional magnetic resonance imaging. Nat Rev Neurosci 8:700–711.

Fries P (2005) A mechanism for cognitive dynamics: Neuronal communication through neuronal coherence. Trends Cogn Sci 9:474–480.

Gray CM, Konig P, Engel AK, Singer W (1989) Oscillatory responses in cat visual cortex exhibit inter-columnar global stimulus properties. Nature 338.

Gupta A, van der Meer M, Touretzky D, Redish D (2016) Segmentation of spatial experience by hippocampal theta sequences. Nat Neurosci 15:1032–1039.

He BJ, Snyder AZ, Zempel JM, Smyth MD, Raichle ME (2008) Electrophysiological correlates of the brain's intrinsic large-scale functional architecture. Proc Natl Acad Sci U S A 105:16039–16044.

Heiduschka P, Schraermeyer U (2008) Comparison of visual function in pigmented and albino rats by electroretinography and visual evoked potentials. Graefe's Arch Clin Exp

Ophthalmol 246:1559–1573.

Honey CJ, Kötter R, Breakspear M, Sporns O (2007) Network structure of cerebral cortex shapes functional connectivity on multiple time scales. Proc Natl Acad Sci U S A 104:10240–10245.

Jacobs GH, Williams G a (2007) Contributions of the mouse UV photopigment to the ERG and to vision. Doc Ophthalmol 115:137–144.

Jones BW, Watt CB, Frederick JM, Baehr W, Chen CK, Levine EM, Milam AH, Lavail MM, Marc RE (2003) Retinal remodeling triggered by photoreceptor degenerations. J Comp Neurol 464:1–16.

Kenyon GT, Moore B, Jeffs J, Denning KS, Stephens GJ, Travis BJ, George JS, Theiler J, Marshak DW (2003) A model of high-frequency oscillatory potentials in retinal ganglion cells. Vis Neurosci 20:465–480.

Kirkby L a, Feller MB (2013) Intrinsically photosensitive ganglion cells contribute to plasticity in retinal wave circuits. Proc Natl Acad Sci U S A 110:12090–12095.

Leopold D a, Murayama Y, Logothetis NK (2003) Very slow activity fluctuations in monkey visual cortex: implications for functional brain imaging. Cereb Cortex 13:422–433.

Lewandowski MH, Błasiak T (2004) Slow oscillation circuit of the intergeniculate leaflet. Acta Neurobiol Exp (Wars) 64:277–288.

Lewandowski MH, Błasiak T, Błasiak A (2002) Are ultra-slow isoperiodic oscillations in rat intergeniculate leaflet neurons dependent on reciprocal connection with its contralaterally located counterpart? Neurosci Lett 330:243–246.

Lewandowski MH, Błasiak T, Domosławski J, Wołkowska a (2000) Ultradian rhythmic neuronal oscillation in the intergeniculate leaflet. Neuroreport 11:317–321.

Lisman JE, Jensen O (2013) The Theta-Gamma Neural Code. Neuron 77:1002–1016.

Lucas RJ, Foster RG (1999) Neither functional rod photoreceptors nor rod or cone outer

segments are required for the photic inhibition of pineal melatonin. Endocrinology 140:1520–1524.

Lucas RJ, Freedman MS, Muñoz M, Garcia-Fernández JM, Foster RG (1999) Regulation of the mammalian pineal by non-rod, non-cone, ocular photoreceptors. Science (80-) 284:505–507.

Lund RD (1964) Uncrossed Visual Pathways of Hooded and Albino Rats. Science (80-) 149:1964–1965.

Menzler J, Zeck G (2011) Network oscillations in rod-degenerated mouse retinas. J Neurosci 31:2280–2291.

Miller JD, Fuller C a (1992) Isoperiodic neuronal activity in suprachiasmatic nucleus of the rat. Am J Physiol 263:R51-8.

Monto S, Palva S, Voipio J, Palva JM (2008) Very slow EEG fluctuations predict the dynamics of stimulus detection and oscillation amplitudes in humans. J Neurosci 28:8268–8272.

Nadal-Nicolás FM, Jiménez-López M, Salinas-Navarro M, Sobrado-Calvo P, Alburquerque-Béjar JJ, Vidal-Sanz M, Agudo-Barriuso M (2012) Whole Number, Distribution and Co-Expression of Brn3 Transcription Factors in Retinal Ganglion Cells of Adult Albino and Pigmented Rats. PLoS One 7.

Orlowska-Feuer P, Allen AE, Storchi R, Szkudlarek HJ, Lewandowski MH (2016a) The contribution of inner and outer retinal photoreceptors to infra-slow oscillations in the rat olivary pretectal nucleus. Eur J Neurosci 43:823–833.

Orlowska-Feuer P, Jeczmien-Lazur JS, Szkudlarek HJ, Lewandowski MH (2016b) Retinal gap junctions are involved in rhythmogenesis of neuronal activity at remote locations – Study on infra-slow oscillations in the rat olivary pretectal nucleus. Neuroscience 339:150–161.

Rao S, Chun C, Fan J, Kofron JM, Yang MB, Hegde RS, Ferrara N, Copenhagen DR, Lang RA (2013) A direct and melanopsin-dependent fetal light response regulates mouse eye

development. Nature 494:243–246.

Renna J, Weng S, Berson D (2011) Light acts through melanopsin to alter retinal waves and segregation of retinogeniculate afferents. Nat Neurosci 14:827–829.

Rodieck R, Smith P (1966) Slow dark discharge rhythms of cat retinal ganglion cells. J Neurophysiol Available at: http://jn.physiology.org/content/jn/29/5/942.full.pdf [Accessed July 6, 2014].

Ryu SB, Ye JH, Goo YS, Kim CH, Kim KH (2010) Temporal response properties of retinal ganglion cells in rd1 mice evoked by amplitude-modulated electrical pulse trains. Investig Ophthalmol Vis Sci 51:6762–6769.

Saleem AB, Lien AD, Krumin M, Haider B, Rosón MR, Ayaz A, Reinhold K, Busse L, Carandini M, Harris KD, Carandini M (2017) Subcortical Source and Modulation of the Narrowband Gamma Oscillation in Mouse Visual Cortex. Neuron 93:315–322.

Smallwood PM, Olveczky BP, Williams GL, Jacobs GH, Reese BE, Meister M, Nathans J (2003) Genetically engineered mice with an additional class of cone photoreceptors: implications for the evolution of color vision. Proc Natl Acad Sci U S A 100:11706–11711 Available at: http://www.pubmedcentral.nih.gov/articlerender.fcgi?artid=208822&tool=pmcentrez&rendertype=abstract.

Storchi R, Bedford RA, Martial FP, Allen AE, Wynne J, Montemurro MA, Petersen RS, Lucas RJ (2017) Modulation of Fast Narrowband Oscillations in the Mouse Retina and dLGN According to Background Light Intensity. Neuron 93:299–307 Available at: http://dx.doi.org/10.1016/j.neuron.2016.12.027.

Szkudlarek HJ, Herdzina O, Lewandowski MH (2008) Ultra-slow oscillatory neuronal activity in the rat olivary pretectal nucleus: comparison with oscillations within the intergeniculate leaflet. Eur J Neurosci 27:2657–2664 Available at:

http://www.ncbi.nlm.nih.gov/pubmed/18547249 [Accessed December 29, 2013].

Szkudlarek HJ, Orlowska P, Lewandowski MH (2012) Light-induced responses of slow oscillatory neurons of the rat olivary pretectal nucleus. PLoS One 7:e33083 Available at: http://www.pubmedcentral.nih.gov/articlerender.fcgi?artid=3299748&tool=pmcentrez&rendertype=abstract [Accessed July 1, 2014].

Trenholm S, Awatramani GB (2015) Origins of spontaneous activity in the degenerating retina. Front Cell Neurosci 9:1–7.

Tsuji T, Tsuji C, Ludwig M, Leng G (2016) The rat suprachiasmatic nucleus: the master clock ticks at 30 Hz. J Physiol 594:3629–3650 Available at: http://doi.wiley.com/10.1113/JP272331.

Vanhatalo S, Palva JM, Holmes MD, Miller JW, Voipio J, Kaila K (2004a) Infraslow oscillations modulate excitability and interictal epileptic activity in the human cortex during sleep. Proc Natl Acad Sci U S A 101:5053–5057.

Vanhatalo S, Palva JM, Holmes MD, Miller JW, Voipio J, Kaila K (2004b) Infraslow oscillations modulate excitability and interictal epileptic activity in the human cortex during sleep. Proc Natl Acad Sci 101:5053–5057.

Zierenberg J, Wilting J, Priesemann V (2018) Homeostatic Plasticity and External Input Shape Neural Network Dynamics. Phys Rev X 8:31018 Available at: https://doi.org/10.1103/PhysRevX.8.031018.

FIGURE LEGENDS

Fig.1 The presence of infra-slow oscillatory activity in the mouse subcortical visual system. A schematic representation of the placement of one 4 × 8 electrode (= 32 recording channels) showing the distribution of recorded units in the A) OPN and B) LGN and whether they were oscillatory. C) Representative firing rate histograms (bin size = 1 s) of spontaneous, dark-adapted activity of infra-slow oscillatory cells in the OPN, dLGN and vLGN (labeled above the histograms). D) FFT analysis performed for the recordings showed in C) classifying cells as infra-slow oscillatory. E) The mean frequency of infra-slow oscillatory activity in the OPN, dLGN and vLGN does not differ between structures (Kruskal-Wallis test, K-W statistics = 5.743, $p = 0.056$). F) The distribution of observed infra-slow frequencies.

Fig. 2 The presence of fast beta/gamma oscillatory activity in the mouse subcortical visual system. A) Fast beta/gamma oscillatory activity continuously observed on a spectrogram. B) ISI histogram (bin size = 0.001 s) computed to confirm existence of harmonic modes in beta/gamma range. C) The mean frequency of fast (beta/gamma) oscillatory activity in the OPN, dLGN and vLGN differs between structures (Kruskal-Wallis test, K-W statistics = 22.12, $p < 0.0001$, Dunn's multiple comparison test). D) The distribution of observed fast frequencies showed that most of them where centered around 30 Hz.

Fig. 3 Types of spontaneous activity in the subcortical visual system. A) Representative firing rate histograms (bin size = 1 s) of spontaneous, dark-adapted activity of different types of oscillatory cells recorded in the dLGN (representative examples). B) FFT and C) PSD analysis were performed to classify cells as infra-slow, fast beta/gamma oscillatory, co-expressing both or none of the above frequencies. D) ISI histograms (bin size = 0.001 s) were computed to confirm existence of harmonic modes in beta/gamma range.

Fig. 4 Infra-slow modulation of fast beta/gamma oscillations in the subcortical visual system of *Opn1mw^R* mice. Representative example of simultaneously recorded activity from

two separate pools of neurons. Firing rate activity has been filtered in the A) infra-slow and B) fast beta/gamma range and normalized as z-score. The color of the lines denote four different phases of the infra-slow rhythm according to the phase quadrants (dark blue: -π to -π/2 radians; dark red: -π/2 to 0 radians; dim red 0 to π/2 radians; dim blue: π/2 to π radians). C) A non-parametric sign-test comparison between fast beta/gamma amplitude recorded during the "red" vs the "blue" phases shows no significant phase modulation. Here the data are grouped across all experiments in which distinct neuronal pools expressing either infra-slow or fast beta/gamma were simultaneously identified. D) and E) are the same as A) and B), respectively, but for a representative example in which a pool of simultaneously recorded neurons co-expressed both infra-slow and fast oscillations. F) Same as panel C but for all experiments in which a population of neurons co-expressing both rhythms was identified. Within these populations the amplitude of fast beta/gamma is significantly modulated by the phase of infra-slow oscillations. G) Statistical comparison between the number of neurons co-expressing infra-slow and fast beta/gamma oscillations that we experimentally observed and the theoretical number predicted by the chance levels and based on the overall number of neurons expressing those two rhythms (either separately or jointly). The number of neurons in which infra-slow and fast beta/gamma are co-expressed is larger than chance across our dataset and in the dLGN and vLGN but not in OPN. The distributions are obtained by using the permutation test as described in Material and Methods section.

Fig. 5 Inner and outer retina contribution to infra-slow and fast beta/gamma oscillatory rhythms emergence. Representative firing rate histograms (bin size = 1 s) of infra-slow oscillatory activity recorded within the dLGN of A) *Opn1mw*^{R}, B) *rd/rd cl* and C) *Opn4*$^{-/-}$ mice. D) Peaks (color coded) correspond to the infra-slow frequency of oscillations presented on A – C, respectively. E) Mean frequency of recorded infra-slow oscillations differs between genotypes in the OPN, dLGN and vLGN. F) The proportion of infra-slow oscillatory cells

differs between the genotypes (Chi-square Test; OPN: $p = 0.0006$, Chi-square statistic = 14.97, df = 2; dLGN: $p < 0.0001$, Chi-square statistic = 45.29, df = 2; vLGN: $p < 0.0001$, Chi-square statistic = 22.17, df = 2). G) Normalized PSDs for two different OPN neurons recorded in *Opn1mw*^{R} and *Opn4*$^{-/-}$ mice (colour coded). H) The mean frequency of fast beta/gamma oscillating neurons differs between *Opn1mw*^{R} and *Opn4*$^{-/-}$ in the OPN and vLGN, but not dLGN. I) The proportion of fast beta/gamma oscillatory cells differs between the genotypes (Chi-square Test; OPN: $p < 0.0001$, Chi-square statistic = 23.13, df = 2; dLGN: $p < 0.0001$, Chi-square statistic = 31.37, df = 2; vLGN: $p < 0.0001$, Chi-square statistic = 21.16, df = 2). Please note, that fast oscillatory cells were not recorded at all in dLGN and vLGN in *rd/rd cl* animals. Data in E analysed by Kruskal-Wallis test followed by Dunn's multiple comparison test; data in H analysed by Mann Whitney (OPN) and Unpaired t-test (dLGN, vLGN); * < 0.05; ** < 0.01; *** < 0.001; **** < 0.0001

Fig. 6 Infra-slow modulation of fast beta/gamma oscillations in the subcortical visual system of *Opn4*$^{-/-}$ mice. Same as Figure 4 but for the *Opn4*$^{-/-}$ dataset.

Fig. 7 Potential circuits mediating infra-slow modulation of fast beta/gamma oscillations. A) The amplitude of fast/beta gamma oscillations is modulated by a distinct population but functionally connected population expressing infra-slow oscillations. B) The same pool of neurons co-express both infra-slow and fast beta/gamma oscillations. The faster rhythm is nested within the slow one.

TABEL LEGEND

Table 1: Permutation Test. The original table contains the data where infra-slow and fast oscillatory expression was detected, the co-expression column tags the units where infra-slow and fast oscillations were co-expressed. The total number of those units is reported as TOTAL COEXP. In the permutation table a random permutation has been applied to the fast column resulting in a different number of units co-expressing both rhythms.

Table 2 Cross-correlation between infra-slow oscillatory neurons, neurons co-expressing infra-slow and fast oscillations and between these two populations. Data was analyzed by sign-test; all p-values < 0.0001 were set at 0; n – number of correlated pairs of neurons. OPN – olivary pretectal nucleus, dLGN – dorsal lateral geniculate nucleus, vLGN – ventral lateral geniculate nucleus, *Opn1mw*^{R} – visually intact mice, *Opn4*$^{-/-}$ - animals lacking melanopsin

Table 3. **Number and proportion of all recorded neurons**. Infra-slow and fast beta/gamma oscillatory activities presented in different structures of the mice subcortical visual system and in different genotypes. OPN – olivary pretectal nucleus, LGN – lateral geniculate nucleus, dLGN – dorsal lateral geniculate nucleus, vLGN – ventral lateral geniculate nucleus, *Opn1mw*^{R} – visually intact mice, *rd/rd cl* – animals lacking rods and cones, *Opn4*$^{-/-}$ - animals lacking melanopsin

FIGURES

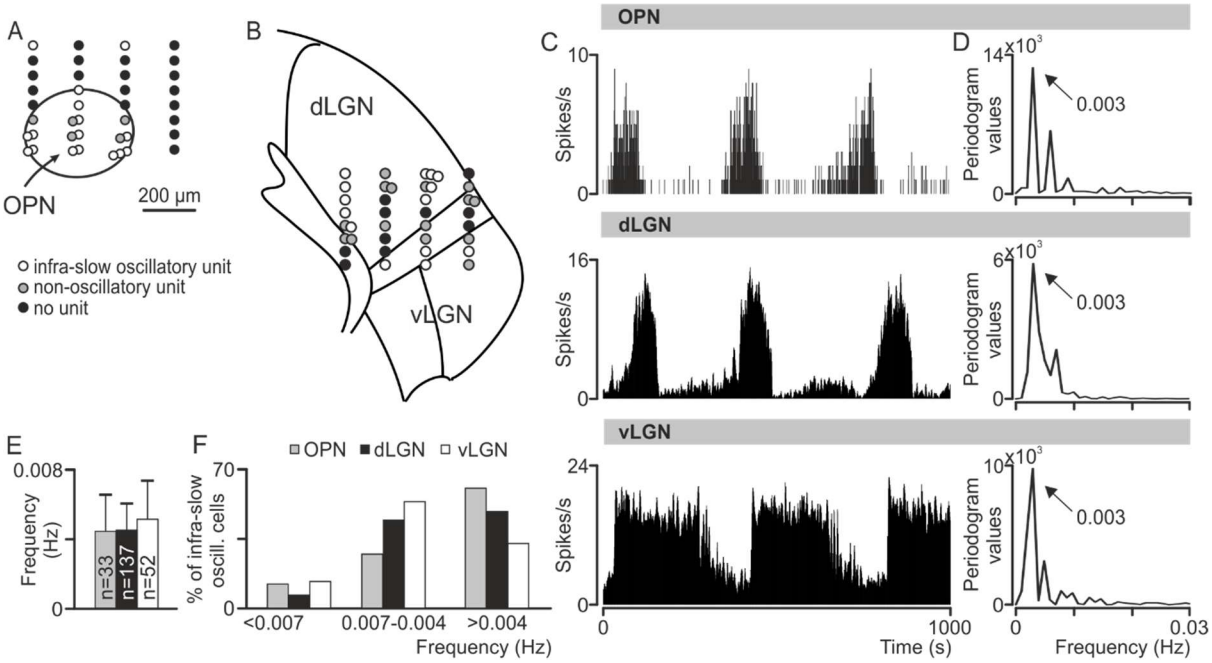

Fig. 1

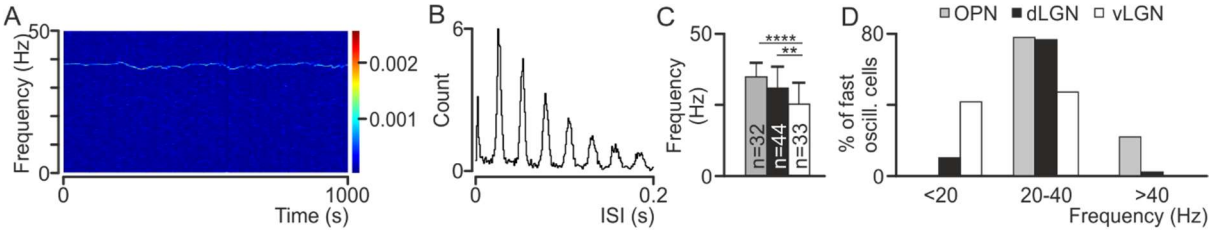
A
Frequency (Hz)
50
0
0
1000
Time (s)
0.002
0.001
B
Count
6
0
0
0.2
ISI (s)
C
Frequency (Hz)
50
0
****
**
n=32
n=44
n=33
D
OPN
dLGN
vLGN
% of fast oscill. cells
80
0
<20
20-40
>40
Frequency (Hz)

Fig. 2

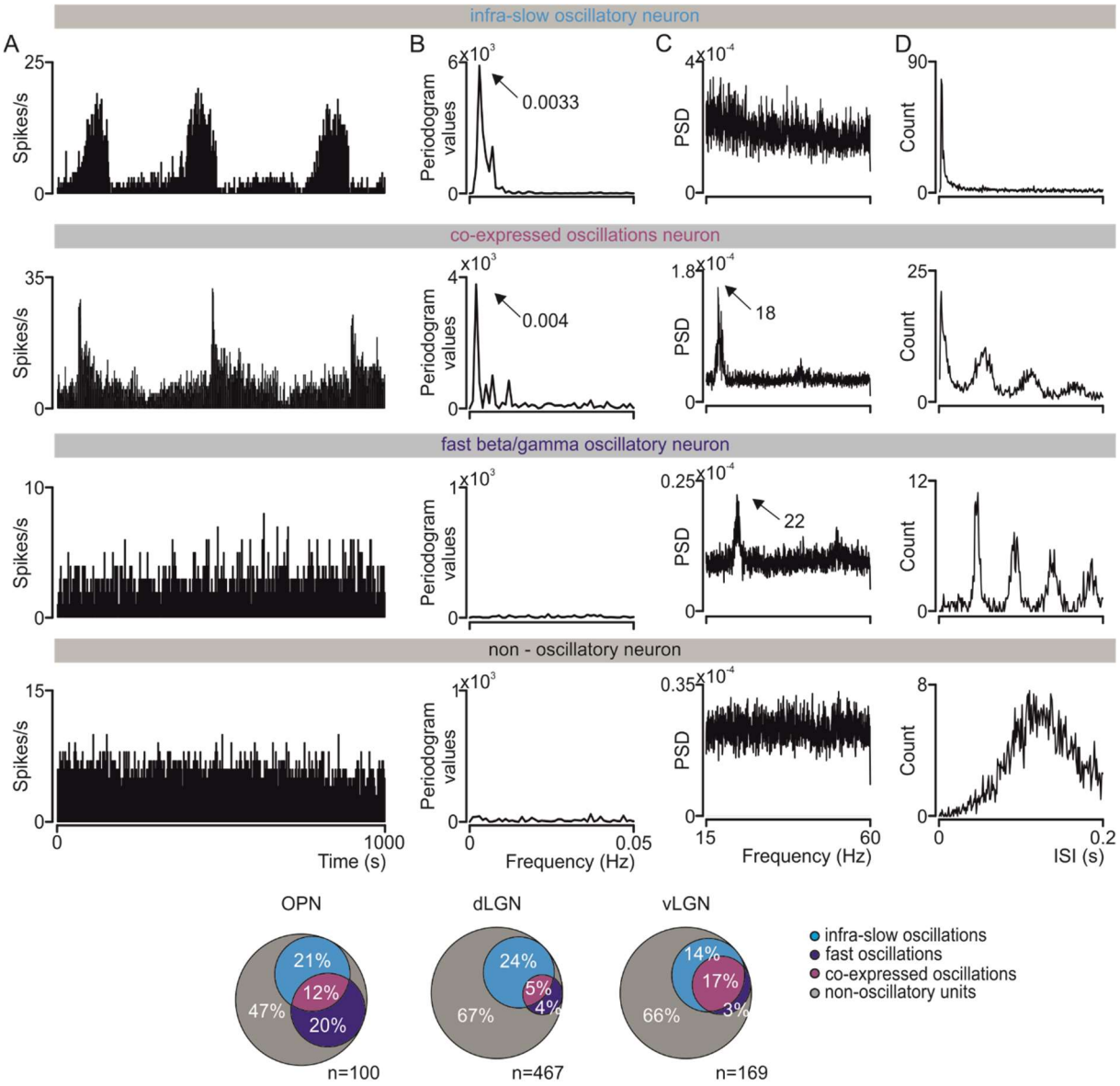
infra-slow oscillatory neuron
A
B
C
D
Spikes/s
Periodogram values
PSD
Count
0.0033
0.004
18
22
Time (s)
Frequency (Hz)
ISI (s)
co-expressed oscillations neuron
fast beta/gamma oscillatory neuron
non - oscillatory neuron
OPN
dLGN
vLGN
21%
12%
20%
47%
n=100
24%
5%
4%
67%
n=467
14%
17%
3%
66%
n=169
infra-slow oscillations
fast oscillations
co-expressed oscillations
non-oscillatory units

Fig. 3

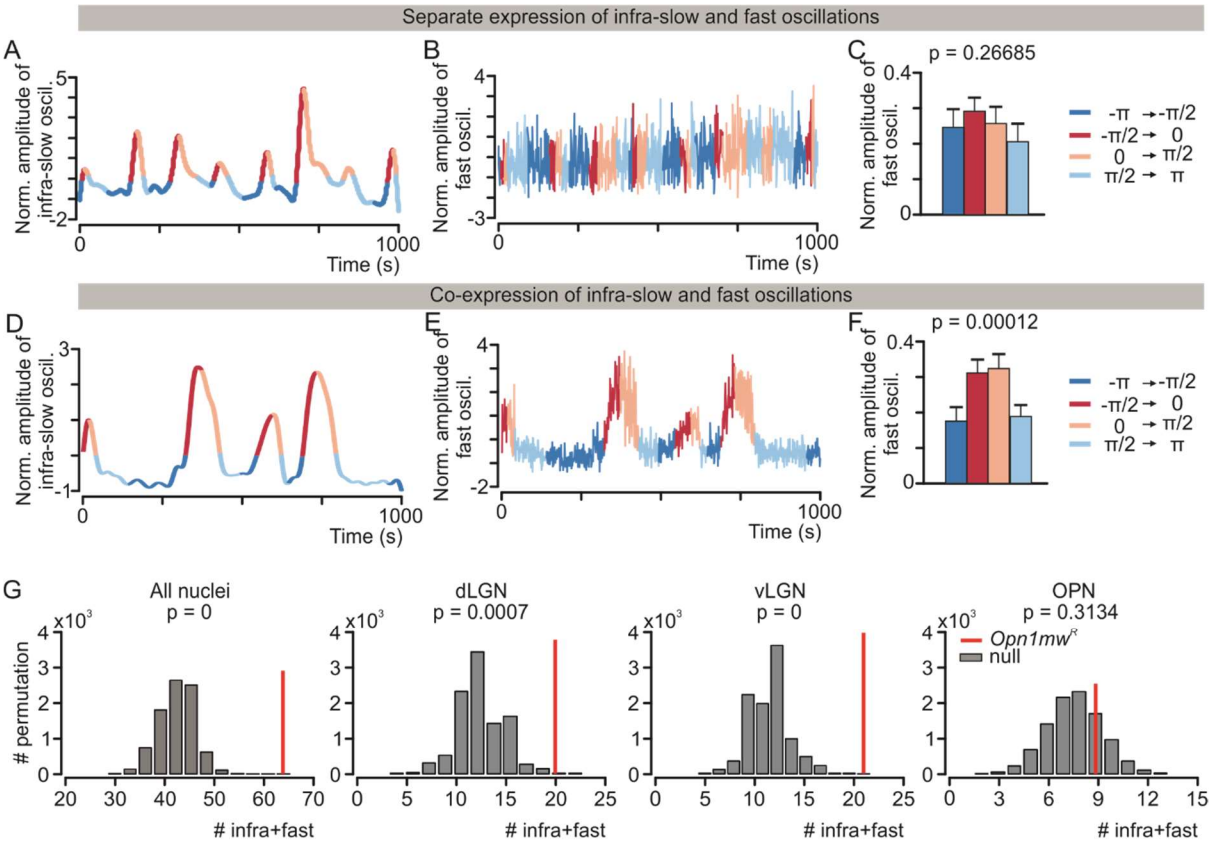
Separate expression of infra-slow and fast oscillations
A
Norm. amplitude of infra-slow oscil.
Time (s)
B
Norm. amplitude of fast oscil.
Time (s)
C
p = 0.26685
Norm. amplitude of fast oscil.
-π → -π/2
-π/2 → 0
0 → π/2
π/2 → π
Co-expression of infra-slow and fast oscillations
D
Norm. amplitude of infra-slow oscil.
Time (s)
E
Norm. amplitude of fast oscil.
Time (s)
F
p = 0.00012
Norm. amplitude of fast oscil.
-π → -π/2
-π/2 → 0
0 → π/2
π/2 → π
G
All nuclei
p = 0
dLGN
p = 0.0007
vLGN
p = 0
OPN
p = 0.3134
Opn1mw^R
null
permutation
infra+fast

Fig. 4

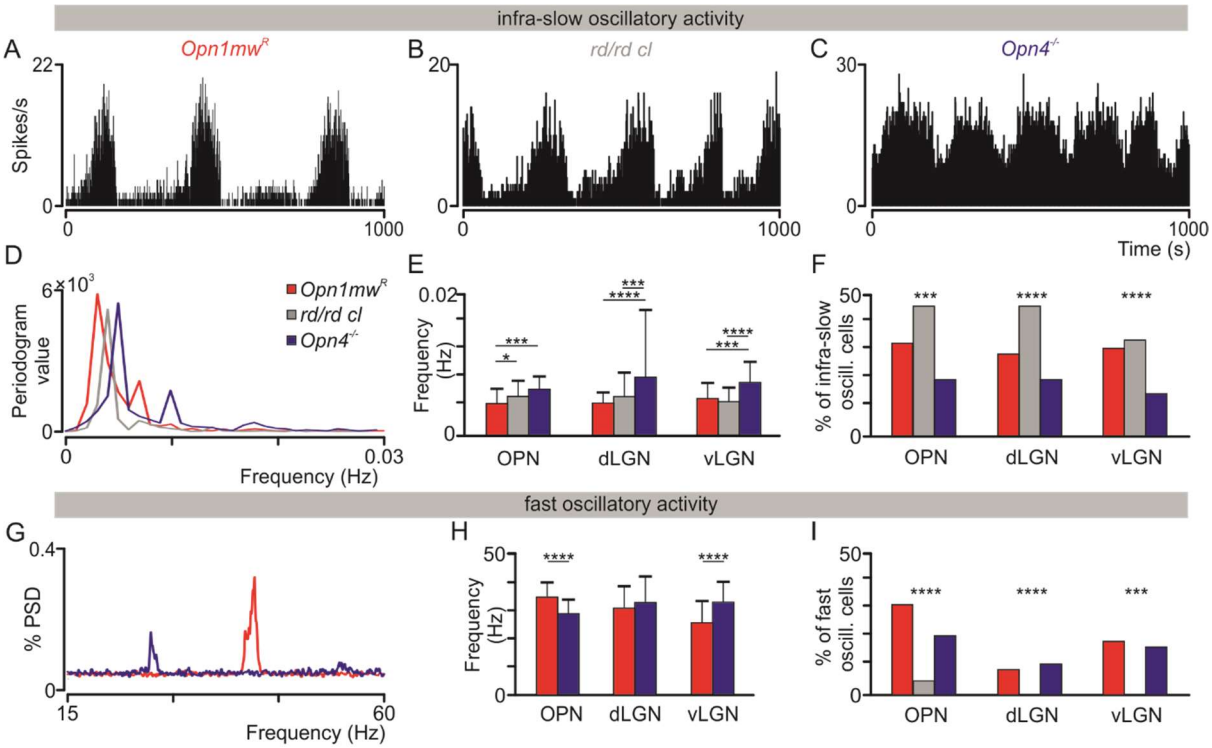
infra-slow oscillatory activity
A
Opn1mw^R
Spikes/s
22
0
0
1000
B
rd/rd cl
20
0
0
1000
C
Opn4^-/-
30
0
0
1000
Time (s)
D
6 ×10^3
Periodogram value
0
0
0.03
Frequency (Hz)
Opn1mw^R
rd/rd cl
Opn4^-/-
E
0.02
Frequency (Hz)
0
OPN
dLGN
vLGN
F
50
% of infra-slow oscill. cells
0
OPN
dLGN
vLGN
fast oscillatory activity
G
0.4
% PSD
0
15
60
Frequency (Hz)
H
50
Frequency (Hz)
0
OPN
dLGN
vLGN
I
50
% of fast oscill. cells
0
OPN
dLGN
vLGN

Fig. 5

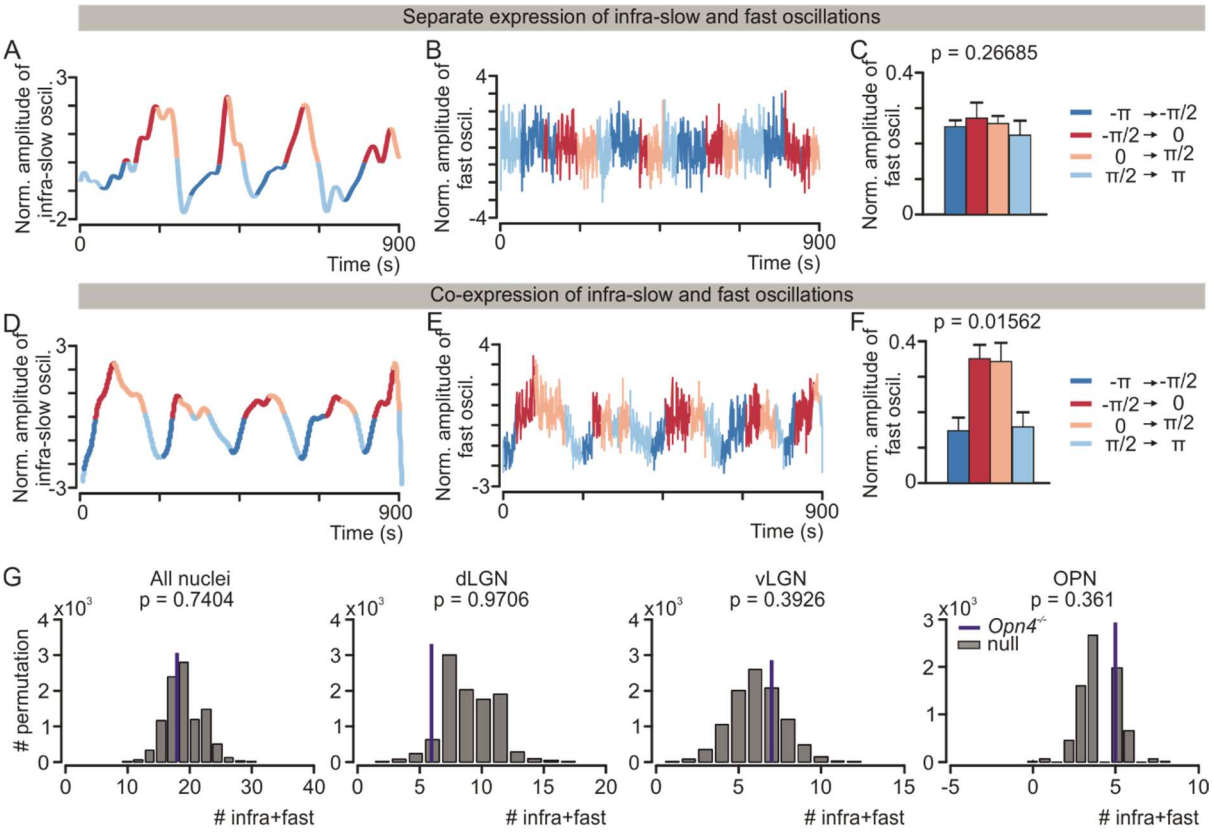
Separate expression of infra-slow and fast oscillations
A
Norm. amplitude of infra-slow oscil.
Time (s)
B
Norm. amplitude of fast oscil.
Time (s)
C
p = 0.26685
Norm. amplitude of fast oscil.
-π → -π/2
-π/2 → 0
0 → π/2
π/2 → π
Co-expression of infra-slow and fast oscillations
D
Norm. amplitude of infra-slow oscil.
Time (s)
E
Norm. amplitude of fast oscil.
Time (s)
F
p = 0.01562
Norm. amplitude of fast oscil.
-π → -π/2
-π/2 → 0
0 → π/2
π/2 → π
G
All nuclei
p = 0.7404
dLGN
p = 0.9706
vLGN
p = 0.3926
OPN
p = 0.361
Opn4-/-
null
permutation
infra+fast

Fig. 6

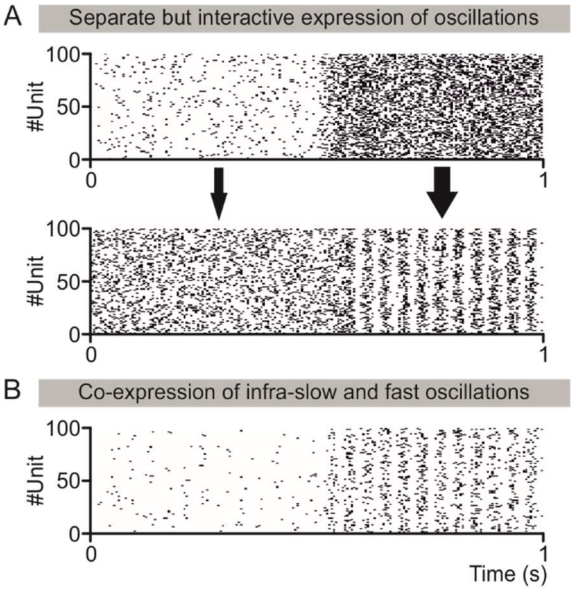
A
Separate but interactive expression of oscillations
100
50
0
#Unit
0
1
100
50
0
#Unit
0
1
B
Co-expression of infra-slow and fast oscillations
100
50
0
#Unit
0
1
Time (s)

Fig. 7

TABELS

Tabel 1

Original Table				Permutation Table			
#unit	Infra-slow	Fast	Co-expression	**#unit**	Infra-slow	Fast	Co-expression
#1	1	0	0	**#1**	1	1	1
#2	1	1	1	**#2**	1	0	0
#3	0	0	0	**#3**	0	0	0
#4	0	0	0	**#4**	0	1	0
#5	1	1	1	**#5**	1	0	0
#6	1	1	1	**#6**	1	0	0
#7	0	0	0	**#7**	0	1	0
#8	1	0	0	**#8**	1	0	0
#9	0	0	0	**#9**	0	0	0
TOTAL COEXP			3	**TOTALCOEXP**			1

Table 2

Structure	**Infra-slow oscillations**		**Co-expressed infra-slow and fast oscillations**		**Between**	
Opn1mw^{R} mice						
	n	p-value	n	p-value	n	p-value
dLGN	658	0	54	0	120	0
vLGN	20	0.0118	109	0	78	0
OPN	41	0.012	19	0	61	0
Opn4$^{-/-}$ mice						
dLGN	193	0	6	0.031	6	1
vLGN	51	0	9	0.004	40	0.268
OPN	5	1	15	0.118	15	0.302

Table 3

	No. of recorded cell			% of infra-slow oscillatory cells			% of fast oscillatory cells		
Genotype	*Opn1mw^{R}*	*rd/rd cl*	*Opn4$^{-/-}$*	*Opn1mw^{R}*	*rd/rd cl*	*Opn4$^{-/-}$*	*Opn1mw^{R}*	*rd/rd cl*	*Opn4$^{-/-}$*
Pretectum (OPN + beyond)	300	364	312	22	38	8	17	3	11
OPN	100	98	75	33	46	20	32	5	21
Pretectum area	200	266	237	19	35	5	8	2	8
LGN (dLGN + vLGN)	636	404	590	30	41	18	12	0.1	13
dLGN	467	307	360	29	43	20	9	0.2	11
vLGN	169	97	230	31	34	15	19	0	17